



Alluvial sequence in the north piedmont of the Chinese Tian Shan over the past 550 kyr and its relationship to climate change

Honghua Lu^{a,b,*}, Douglas W. Burbank^c, Youli Li^b

^a State Key Laboratory of Marine Geology, Tongji University, Shanghai 200092, China

^b Key Laboratory of Earth Surface Processes of Ministry of Education, Peking University, Beijing 100871, China

^c Department of Earth Science, University of California at Santa Barbara, California 93106, USA

ARTICLE INFO

Article history:

Received 26 May 2009

Received in revised form 13 November 2009

Accepted 22 November 2009

Available online 30 November 2009

Keywords:

Fluvial terrace

Alluvial fan

Loess/paleosol sequence

Climate change

Tian Shan

ABSTRACT

A new division of Middle and Late Pleistocene alluvial sequence in the north piedmont of the Chinese Tian Shan based on geomorphologic, stratigraphic, and chronologic criteria provides a framework for examining their relationship to climate change during glacial–interglacial transitions. Over the past 550 kyr at least four major alluviation episodes occurred within the piedmont. Along the major river valleys in this region, each episode of alluvial fan deposition morphologically correlates with a major river terrace. These correlations create a regionally applicable framework for subdivision of the Quaternary alluvial sequence in the study area, where seven stepped river terraces are defined. Our new chronology of this fluvial sequence suggests that, following intervals of aggradation, three highest river terraces and equivalent alluvial fans were abandoned at ~530 ka, ~300 ka and ~10 ka, respectively. Paleosols at the base of the loess sequences that directly overlie the older terraces and fans suggest that episodes of aggradation occurred late in the glacial cycles. The subsequent incision that caused abandonment/stabilization of these terraces and fans occurred near to glacial–interglacial transitions. A relatively high degree of synchrony in major river incision events across the piedmont, despite disruption by several discrete structure zones with asynchronous tectonic activities, supports the dominant control exerted by climatic conditions on alluvial deposition and terrace creation during the Quaternary across the north piedmont of the Chinese Tian Shan.

© 2009 Elsevier B.V. All rights reserved.

1. Introduction

Many studies have illustrated the importance of alluvial sequences in tracking past changes in climate and regional tectonics (e.g., Avouac et al., 1993; Avouac and Peltzer, 1993; Molnar et al., 1994; Pinter et al., 1994; Li et al., 1996, 1999; Li and Yang, 1997; Yang et al., 1998; Hanson et al., 2006; Scharer et al., 2006; Westaway et al., 2006). Controversy persists, however, about whether stepped alluvial sequences derive basically from climatic variations during glacial–interglacial transitions (Macklin et al., 2002; Pan et al., 2003; Bridgland and Westaway, 2007), tectonic uplift (Lu et al., 2004; Sun, 2005), or other nonglacial/nontectonic factors such as monsoon intensification (Pratt et al., 2002). Even for the same geomorphic feature, various workers sometimes interpret the forcing mechanism in a different way as tectonic uplift or climate change during the glacial–interglacial cycles. The Tian Shan and its surrounding area provide a natural laboratory to probe this scientific question.

The modern Tian Shan has been built largely by basinward thrusting along faults that branch from the reactivated, relatively

steeply dipping, range-bounding Junggar Frontal Thrust fault (Molnar and Tapponnier, 1975; Avouac et al., 1993; Lu et al., 2009). The present topography of the north piedmont of the Tian Shan is characterized by several roughly east–west-trending zones of fault-related folds (Avouac et al., 1993; Burchfiel et al., 1999; Fu et al., 2003) (Fig. 1b). Transverse rivers incise into the anticlines roughly perpendicular to their strike and display well-developed alluvial fans and fluvial terrace sequences. Since the pioneering studies in the 1960s on the alluvial units in the north piedmont of the Tian Shan in northwestern China, e.g., Liu and Zhang, 1962; Zhou, 1963; Liu, 1965, most subsequent studies of these alluvial sequences have focused largely on their neotectonic significance (e.g., Xu et al., 1992b; Avouac et al., 1993; Zhang et al., 1994; Yang et al., 1995; Shi et al., 2004; Yuan et al., 2006), whereas relatively few studies (e.g., Molnar et al., 1994; Zhang et al., 1995) have focused on the geomorphic processes that controlled their formation. Moreover, most of these previous studies were conducted either only within the anticlines in the northern Tian Shan piedmont or along individual river systems, and consequently they failed to temporally compare the morphologic sequences of different river systems. As a result, some ambiguity persists concerning correlation of the Quaternary fluvial geomorphologic succession across this region. Moreover, for those terraces that have been dated (e.g., Molnar et al., 1994; Zhang et al., 1995; Wang and

* Corresponding author. Rm. 517, Ocean Building, Tongji University, No. 1239 Siping Rd., Shanghai 200092, China. Tel.: +86 21 6598 4906.

E-mail address: lvhh2008@163.com (H. Lu).

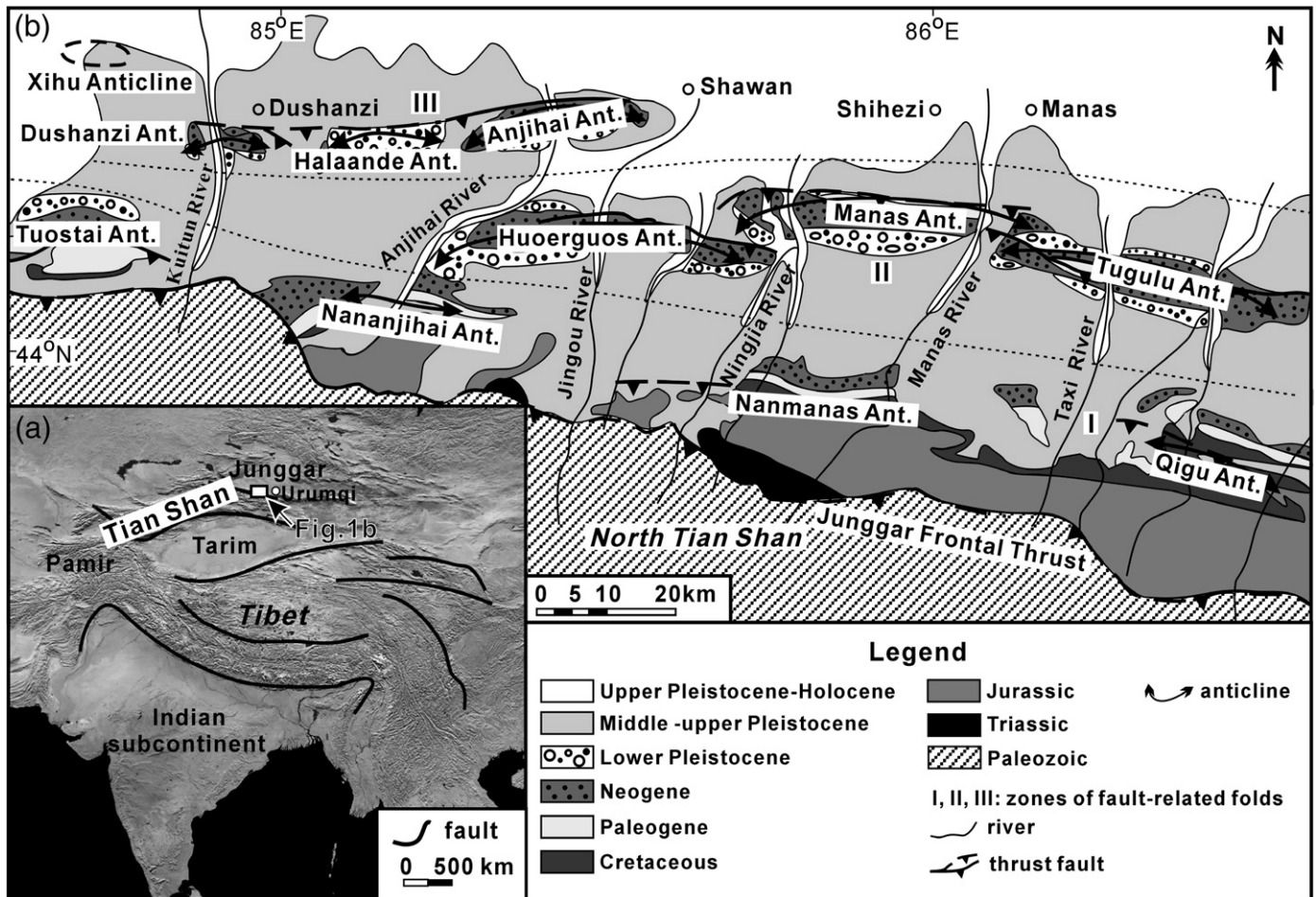


Fig. 1. (a) General structural setting in central Asia. (b) Map depicting generalized geology of the northern flank of the Tian Shan, northwestern China (modified from Zhang et al., 1994).

Wang, 2000; Yuan et al., 2006), inconsistent ages impede correlations of the alluvial sequence to documented climatic or tectonic events.

In order to obtain a more complete picture of the Quaternary alluvial geomorphologic evolution along the north flank of the Chinese Tian Shan, we focused on four major river systems (Anjihai River, Jingou River, Manas River, and Taxi River) (Fig. 1b). Along these rivers, we have studied 26 terrace cross-sections and two representative loess sections. From these, we have dated nine samples from eight different sites using electron spin resonance (ESR) and optically stimulated luminescence (OSL) dating. The goals of this paper are (1) to describe the distribution and episodes of alluvial fan deposition, (2) to define the fluvial terrace sequence, and (3) to evaluate the possible contribution of climate change and/or tectonic deformation to alluvial deposition and river incision. Despite an actively tectonic regime in the north piedmont of the Tian Shan (e.g., Avouac et al., 1993; Molnar et al., 1994; Burchfiel et al., 1999), our new chronology extends through at least six glacial-interglacial cycles and suggests that favorable climatic conditions, rather than tectonics, promoted the formation of most Quaternary alluvial geomorphology in this region.

2. Geological setting

As one of the largest and most active mountain ranges in Asia, the east-west-trending Tian Shan exhibits high current seismicity and rapid rates of Neogene deformation (Abdrakmatov et al., 1996; Reigber, et al., 2001). In response to north-south convergence driven by the India-Asia collision during the Cenozoic times (Molnar et al., 1993; Tapponnier et al., 2001), the ancestral Tian Shan has been

reactivated. As a consequence, several successive zones of fault-related folds have developed within both the northern and southern Tian Shan foreland (e.g., Avouac et al., 1993; Burchfiel et al., 1999; Fu et al., 2003; Lu et al., 2009). Thick Mesozoic and Cenozoic terrigenous strata were exhumed and eroded in the cores of these folds (e.g., Charreau et al., 2005, 2006; Chen et al., 2007; Heermance et al., 2007; Lu et al., 2009). We focus on the north piedmont of the range, where such three zones (known as zones I to III) characterize the regional topography and stretch from the mountain front sequentially towards the foreland basin (Fig. 1b). Most of anticlines in these structural zones comprise Cenozoic depositional strata, except for some anticlines of zone I that expose both Mesozoic and Cenozoic strata (Fig. 1b). Along a traverse from the proximal to distal structure zones, growth strata and unconformities chronologically constrain their initial growth to range sequentially from Miocene to Mio-Pliocene to latest Early Pleistocene (Xu et al., 1992a; Burchfiel et al., 1999; Deng et al., 2000; Lu et al., 2009).

Most of rivers in the piedmont of the north Tian Shan originate from active glaciers in the axial parts of the range. With annual precipitation <300 mm/yr in the piedmont, the fluvial water supply depends strongly on snow melt, and displays strong seasonal variations in discharge. Similarly, sediment transport, discharge, and erosional competency of these river systems likely varied during past glacial and interglacial periods. Quaternary alluvial units preserved along these piedmont river systems can serve to clarify the relationship of their stratigraphy and morphology with past climate change and/or tectonism (Avouac et al., 1993; Molnar et al., 1994). Pleistocene loess extensively mantles several high terrace and fan

surfaces, as well as dissected anticlines in the north piedmont of the Tian Shan (Zhang, 1981; Deng et al., 2000). Although the Tian Shan loess deposits lack the detailed resolution and correlation potential of analogous sequences in the Chinese Loess Plateau, the correlations between them have been tentatively made and appear persuasive (e.g., Zhang, 1981; Fang et al., 2002). Controlled by both north–west and north–north–east winds (Fang et al., 2002), the Tian Shan loess deposits thicken and then thin northward from the mountain front towards the foreland basin. The thickest loess/paleosol sequence consequently occurs in the area between Taxi River and Jingou River (Xinjiang Institute of Geography, 1986).

3. Methods

In order to improve the temporal and geomorphologic framework of the Quaternary alluvial sequence in the north piedmont of the Tian Shan and to examine how alluvial variations relate to climate change and/or tectonic movement, our analysis comprises three principal facets: geomorphologic surface dating; loess–paleosol correlation; and synthesis of the geomorphologic succession.

3.1. Geomorphologic surface dating

Well-constrained chronologies for Quaternary deposition and erosion underpin tests of synchrony among potentially coeval fan and terrace surfaces in different valleys. Previous studies (e.g., Zhang et al., 1995; Wang and Wang, 2000) suggest that the ages of some terraces in the northern Tian Shan foreland lie beyond the typical range of conventional radiocarbon dating (i.e., 45 ka). Our age control for these geomorphologic units is, therefore, based primarily on both electron spin resonance (ESR) and optical stimulated luminescence (OSL) dating. ESR and OSL samples were collected from homogeneous fluvial sediments or loess deposits. When sampling, a 20-cm-long, 5-cm-diameter steel pipe with one end covered with opaque materials was driven into the sampled layer using a plastic hammer. Five ESR samples and four OSL samples were taken at eight different sites (Fig. 2). In order to insure maximal shielding, we analyzed only the middle part of each sample. Based on samples that comprise silt or very fine sand and following the procedures of Lin et al. (2005), Rees-Jones (1995), and Wang (2006), respectively, ESR and OSL dates were determined in the State Key Laboratory of Earthquake Dynamics, Institute of Geology, China Earthquake Administration.

3.2. Loess/paleosol stratigraphic correlation

Because many fans and terraces in the study region are capped by loess/paleosol sequences, we used magnetic susceptibility of these successions to estimate a minimum age for the underlying geomorphologic surfaces. These independent analyses also provide a framework for comparison to the associated ESR and OSL dates. Previous studies, e.g., Liu (1985), have subdivided the loess/paleosol sequence in the Loess Plateau, north China into successive climato-stratigraphic units (loess units: L_1, L_2, \dots ; paleosol units: S_1, S_2, \dots). Because each recognized loess or paleosol unit can be used as a distinctive regional stratigraphic horizon of a known age, these successions serve as dating tools in roughly the same way as the marine oxygen–isotope record can be used to correlate Quaternary sediments in deep-sea cores (Fig. 3). Moreover, the loess/paleosol sequence is well established as a continuous terrestrial record of climate change spanning more than two million years (Liu, 1985; An et al., 1990; Ding et al., 1994): loess accumulates during relatively cold and dry periods, and paleosols develop in relatively wet and warm episodes (Liu, 1985; Kukla et al., 1988; An et al., 1990, 1991).

Two representative loess sections, Lujiaowan (LJW) and Hankazi (HKZ) sections (Figs. 2, 4 and 5), were systematically analyzed. The identification of the loess/paleosol units was based on their distinctive

physical characters (e.g., texture, structure, color, thickness, and magnetic susceptibility), as well as their stratigraphic position in the regional sequence. Magnetic susceptibility was measured at vertical sampling intervals of 5 cm throughout each section. In comparison to the classic loess/paleosols sequences of the Loess Plateau in north China (Liu, 1985), the paleosols in the arid Tian Shan study area are significantly attenuated and produce a spiky susceptibility peak, rather than a somewhat broad peak associated with thicker paleosols where they are better developed. Although the loess deposits in the north piedmont of the Tian Shan are not as regionally uniform as those in the Loess Plateau, their magnetic susceptibility records and associated ESR dates can be quite convincingly correlated among them in order to identify the stratigraphic equivalent of each loess/paleosol layer and to estimate an approximate age for each loess/paleosol unit (Figs. 3 and 5).

3.3. Definition of the geomorphologic sequence

A four-step process is used to define the geomorphic sequences in the study area. First, for each geomorphic feature (alluvial fan and terrace), field observations define the geomorphic surface's elevation, the bedrock beneath it, the thickness of capping gravels and overlying loess, and the succession of paleosols (if any) within the loess. Second, we utilize 1:50,000 topographic maps, field investigations, and geomorphologic mapping based on Landsat TM imagery to establish the sequence of alluvial fans and fluvial terraces along each river system. Third, based on the topographic continuity, the surface characteristics of the alluvial fans and terraces, and the ages of those surfaces, we develop correlations of the four episodes of alluvial fan development (F_1 to F_4) with four major river terraces (T_1, T_2, T_3 and T_6) within the piedmont. Fourth, on the basis of these correlations, we compare the alluvial sequences among the individual river systems in the north piedmont of the Tian Shan and classify seven river terraces (T_1 to T_7 from oldest to youngest) and their relative alluvial fan sequences.

4. Quaternary alluvial geomorphology sequence

4.1. Four episodes of alluvial fan deposition

Extending across the sub-parallel, east–west-trending zones of fault-related folds in the northern Tian Shan foreland, north-flowing rivers display well-developed alluvial fans (Fig. 2) that can be assigned to four distinct depositional episodes (F_1, F_2, F_3 , and F_4). These episodes occur sequentially from hinterland to foreland (Fig. 2) and are distinguished from each other on the basis of their topographic continuity, fan morphology, surface characteristics, and the overlying loess/paleosol sequences.

The oldest alluvial fan (F_1) is best expressed along the margins of Manas River (Fig. 2), where it is mainly preserved in the proximal part of the foreland, as well as along both flanks of the Tugulu anticline: the outermost large fold along this transect. The F_1 fan surface is incised by gullies and thus exists as a heavily dissected and undulating terrain. The proximal part of this fan is tilted toward the north with steep gradients, and its surface merges northward with the next younger and much gentler fan. The alluvial deposits of the F_1 fan are composed of blackish gray gravel more than 20 m thick in many places. In some places, eolian loess deposits commonly about 20–40 m thick overlie the F_1 fan deposits, especially in the more distal areas. A representative loess section, e.g., the Hankazi section (Figs. 2 and 4a), commonly displays five paleosol units which contain sparse fragments of calcareous nodules (Fig. 5a). The lowest brown paleosol layer is the most clearly expressed, whereas the other four paleosol layers are nearly undistinguishable due to the relatively weaker pedogenesis. The magnetic susceptibility profile shows five intervals with relatively higher magnetic susceptibility (Fig. 5a). When

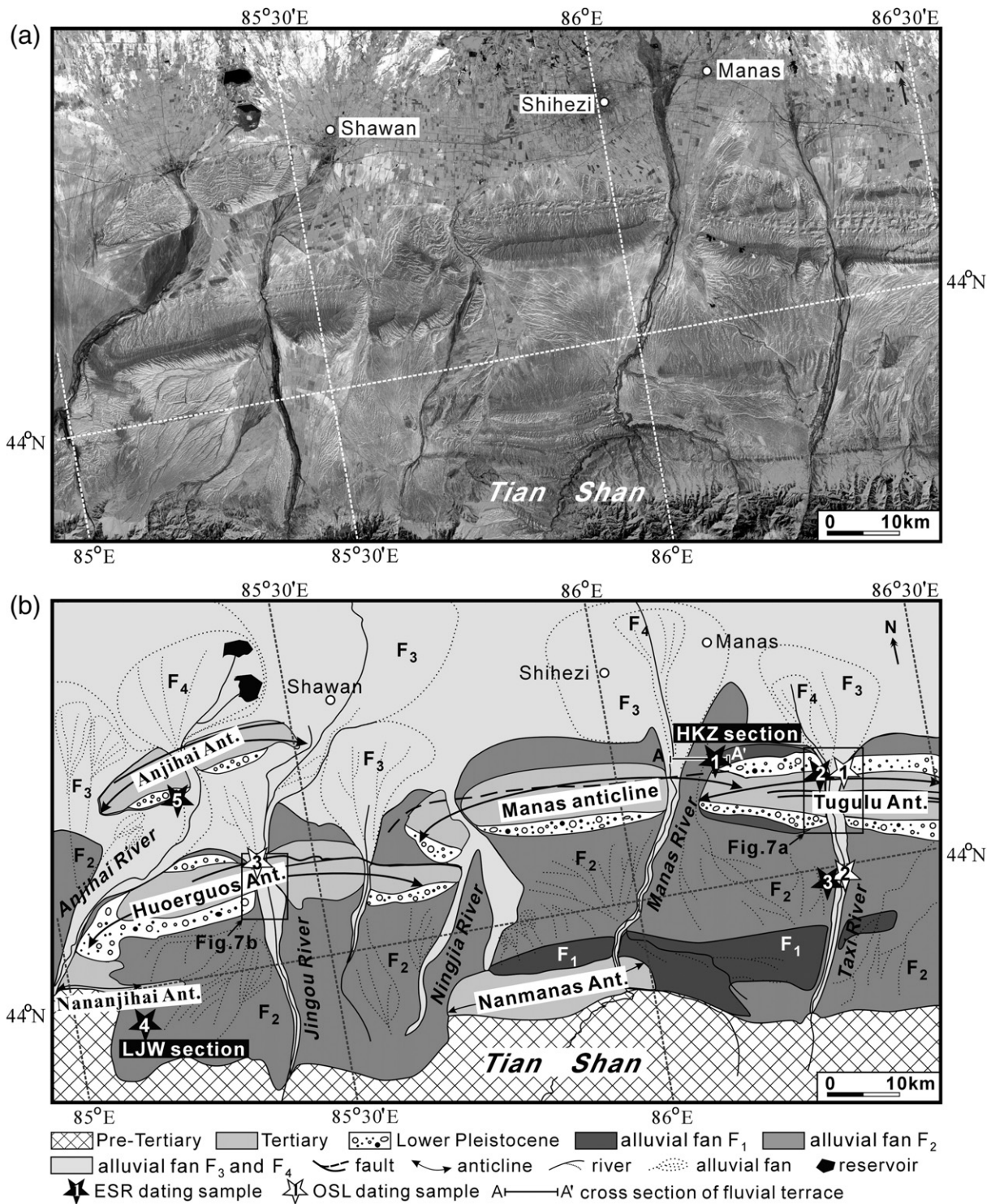


Fig. 2. (a) Landsat TM image and (b) geological interpretative map showing the distribution of geomorphic surfaces in the northern Tian Shan foreland along with locations of some research sites discussed in the text. Solid and open stars show the sampling sites for ESR and OSL dating, respectively, as reported in Tables 1 and 2. LJW—Lujiaowan, HKZ—Hankazi.

compared with the magnetic susceptibility curve from the Chinese Loess Plateau (Kukla et al., 1988) (Fig. 5c), we deduce that these five layers are S_1 to S_5 , respectively (Fig. 5a). S_5 is one of the most striking paleosol units in the Chinese Loess Plateau, where it is further subdivided to paleosol units S_{5a} , S_{5b} , and S_{5c} (Fig. 3) which are estimated to span from 470 to 610 ka and correlate to Marine Isotope Stages 13 to 15 (Fig. 3). Given the ESR age of 537 ± 56 ka from the lowest and best-developed paleosol layer in the Hankazi section (Fig. 5a and Table 1) and the five susceptibility peaks in the overlying

loess/paleosol succession, we interpret this Hankazi paleosol to correspond with paleosol S_{5a} in the Loess Plateau where it dates from ~470–530 ka (Fig. 3). This correlation implies that paleosols S_{5b} and S_{5c} , corresponding to Marine Isotope Stage 15a and b (Fig. 3), are not present at Hankazi and that both the cessation of the correlative F_1 alluvial-fan deposition and the base of the loess sequence approximate the stage 13/14 transition at ~530 ka (Figs. 3 and 5).

The distribution of the next younger alluvial fan (F_2) is the most extensive among all the alluvial fans in the study area (Figs. 2 and 4c)

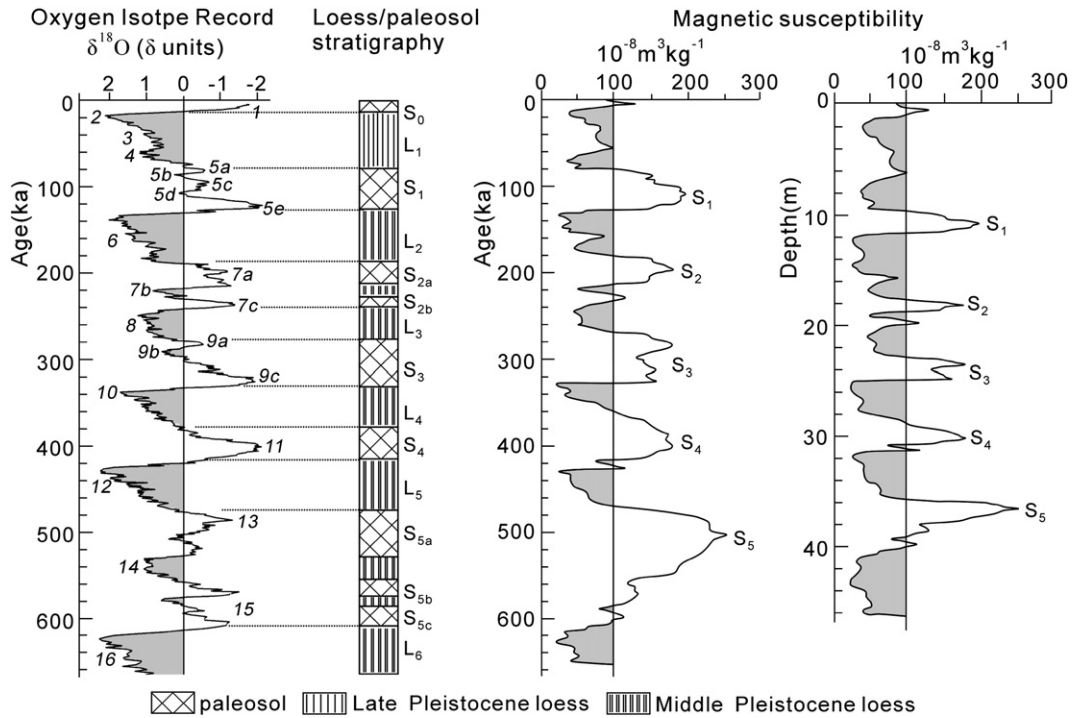


Fig. 3. Correlation of the oxygen–isotope record (Lisiecki and Raymo, 2005) with the Chinese loess/paleosol stratigraphy over the last 600 kyr (Liu, 1985). The profile of magnetic susceptibility is shown for loess section at Luochuan, Loess Plateau, north China (Kukla et al., 1988).

and is largely developed to the south of structure zone II (Fig. 2). The fan surface is incised by gullies commonly up to depth of several meters (Fig. 4c), but is less incised than F_1 . In both the northern and southern limbs of anticlines, the F_2 fan surface is distinctly tilted by Late Pleistocene folding, as revealed by the deformed river terraces (T_2) that correlate with F_2 . F_2 alluvial deposits are composed of blackish gray gravel, commonly thickening within synclines and

thinning across anticlines, as is typical for growth strata (Suppe et al., 1992). Deposition within synclines likely buried the earlier alluvial sediments, thus resulting in the discontinuous outcrop distribution of F_1 . Where preserved, the loess/paleosol stratigraphy overlying the F_2 gravels is commonly thinner than that on the F_1 gravels: about 10–20 m thick. A representative loess section located at Lujiawowan (Figs. 2 and 4b) clearly contains three brown paleosol units with sparse

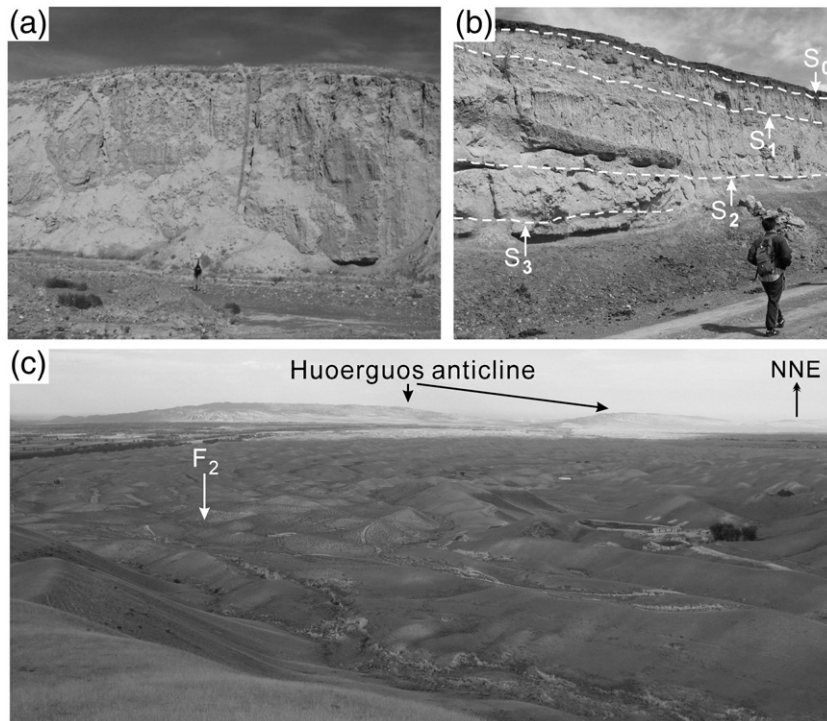


Fig. 4. Photographs showing the loess deposits overlying the gravels of alluvial fans F_1 and F_2 . (a) Hankazi (HKZ) loess section; (b) Lujiawowan (LJW) loess section; (c) the alluvial fan F_2 to the south of Huoerguos anticline displaying its wavy surface. Each person in (a) and (b) is ~170 cm tall. See Fig. 2 for the locations of sections (a) and (b).

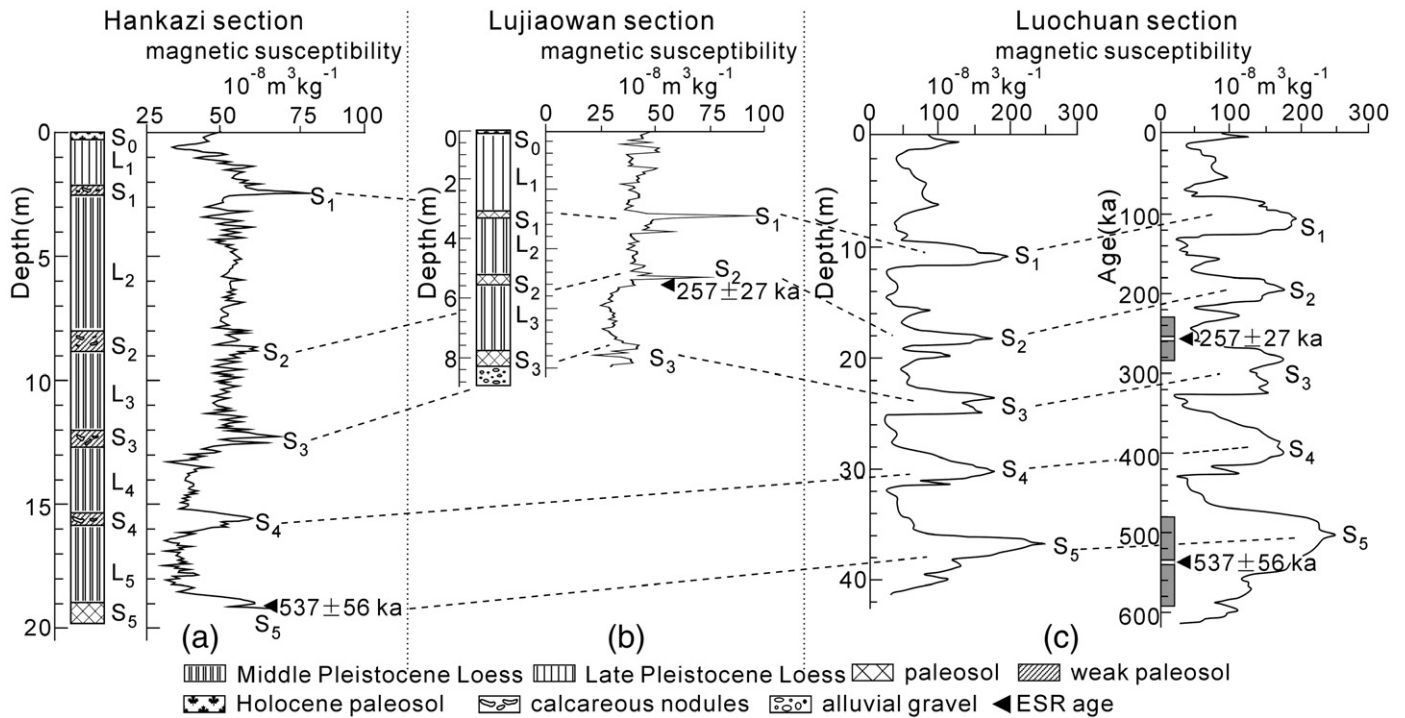


Fig. 5. Correlations of magnetic susceptibility profiles from Hankazi (a) and Lujiawan (b), in the northern Tian Shan foreland with the result from Luochuan (c), Chinese Loess Plateau (Kukla et al., 1988). Note that the depth section of susceptibility at Luochuan (left column) is more “spiky” than the time section (right column) and more similar to the Hankazi and Lujiawan susceptibility curves. ESR ages in the Hankazi and Lujiawan sections are also depicted in the Luochuan time section to reinforce the correlations among them. Hankazi and Lujiawan loess sections rest on the gravels of terraces T_1 (F_1) and T_2 (F_2), respectively. See Fig. 2 for the locations of sections (a) and (b).

calcareous nodules (Figs. 4b and 5b) that can be readily distinguished from intervening yellow loess deposits. All the paleosol layers are less than 0.5 m in thickness. The lowest paleosol layer directly overlies the alluvial gravel. Based on the ESR date of 257 ± 27 ka (Table 1) taken from the second paleosol unit and the correlation of the magnetic susceptibility curve of the Lujiawan section with the result from Chinese Loess Plateau (Kukla et al., 1988) (Fig. 5c), the lowest paleosol is inferred to be S_3 , and its age is estimated to be ~ 280 – 320 ka (Fig. 3), thereby suggesting that the alluvial deposition of F_2 at Lujiawan had ended by ~ 300 ka. On the southern limb of Anjihai anticline, an ESR age of 288 ± 28 ka for a sample taken from the base of loess overlying the F_2 alluvial deposits (Table 1 and Fig. 2) constrains the cessation of the F_2 fan deposition of Anjihai River at about the same time: ~ 300 ka. In the eastern part of the study area, two ESR samples (samples 2 and 3, Table 1 and Fig. 2) taken from the lower part of loess sediments sitting on the F_2 deposits on opposite flanks of the Tugulu anticline along Taxi River are dated at ~ 210 ka. Based on the above correlations of the local loess stratigraphy to the well-established ages of the loess–paleosol sequence in the Loess Plateau (Fig. 5), we estimate average sediment-accumulation rates of Pleistocene loess in the Hankazi and Lujiawan sections in the study area to be ~ 36 mm/kyr and ~ 27 mm/kyr, respectively: a consistency in rates demonstrates in

turn the rationality of our loess/paleosol stratigraphic correlations. When combining with the thickness of ~ 2.0 or ~ 3.0 m between the sampling level and the top of alluvial gravels at ESR sampling sites 2 and 3, we can estimate an age of ~ 270 to 320 ka for the cessation of the F_2 fan deposition of Taxi River. Together, the ESR ages (Fig. 2 and Table 1) and the loess/paleosol stratigraphic correlation (Fig. 5) constrain abandonment of the aggradational surface of the alluvial fan F_2 across the piedmont of the north Tian Shan at about 300 ka. Given the ~ 100 -km-long swath of the northern Tian Shan foreland (Fig. 2), however, the limited number of dated samples (four ESR ages) creates some uncertainties in both the identification and age of the fan F_2 . Further dating should focus on the middle part of the study area (such as Ningjia River and Manas River, Fig. 2).

The younger alluvial fans (F_3 and F_4) developed mainly in the distal fringes of structural zones II or III of fault-related folds (Fig. 2). The surface of alluvial fan F_3 is planar with little post-deposition incision and lacks loess deposits: all features in striking contrast with the two oldest fans. OSL ages from Jingou River and Taxi River (Table 2 and Fig. 8c), together with age data from previous studies (Molnar et al., 1994; Yuan et al., 2006), indicate that F_3 developed mainly during the range from ~ 30 to ~ 10 ka. Stabilization of alluvial fan F_4 is inferred at the beginning of Holocene.

Table 1

Calculated value of equivalent doses, annual doses, and ESR ages.

Sample no.	Sampled layer	Dating material	Equivalent doses (Gy)	Annual doses (Gy/kyr)	ESR age (ka)
1	S_5 in the Hankazi loess section overlying F_1 (T_1) alluvial gravels of Manas River (see Fig. 5a)	Silty clay	1854 ± 195	3.45	537 ± 56
2	Lower part of loess deposits overlying F_2 (T_2) alluvial deposits of Taxi River, on the north limb of Tugulu anticline	Silt	680 ± 68	3.26	209 ± 20
3	Lower part of loess sediments overlying F_2 (T_2) of Taxi River, to the south of Tugulu anticline	Silt	700 ± 70	3.19	219 ± 21
4	S_2 in the Lujiawan loess section sitting on alluvial gravels of F_2 (T_2) (see Fig. 5b)	Silty clay	869 ± 90	3.37	257 ± 27
5	The base of loess overlying F_2 (T_2) of Anjihai River	Silt	1124 ± 112	3.9	288 ± 28

Locations of ESR samples No.1 to No.5 are shown with solid stars in Fig. 2.

The age uncertainty is 1σ .

Table 2

Calculated values of equivalent doses, annual doses, and OSL ages.

Sample no.	Sampled layer	Height above river (m)	Dating material	Equivalent doses (Gy)	Annual doses (Gy/kyr)	OSL age (ka)
1	Top of T_7 of Taxi River on the north limb of Tugulu anticline	~5	Silt	6.7 ± 0.3	3.8 ± 0.4	1.8 ± 0.2
2	Base of T_3 (F_3) alluvial deposits of Taxi River to the south of Tugulu anticline	~110	Silt	109.7 ± 3.0	4.2 ± 0.4	26.0 ± 2.7
3a	Base of T_3 (F_3) alluvial deposits of Jingou River (see Fig. 8c)	~41	Silt	130.5 ± 4.2	4.5 ± 0.5	28.7 ± 3.0
3b	Top of T_3 (F_3) alluvial sediments of Jingou River (see Fig. 8c)	~51	Silt	49.5 ± 0.8	3.9 ± 0.4	12.6 ± 1.3

Locations of OSL samples No.1 to No.3 are shown with open stars in Fig. 2. The age uncertainty is 1σ .

4.2. Fluvial sequence of seven terraces

Field investigations indicate that main terrace surfaces (T_1 , T_2 , T_3 , and T_6) grade laterally or downstream into the surfaces of the alluvial fans discussed above (Figs. 6 and 7). These correlations, therefore, define a geomorphologic framework that provides a useful tool for comparing the terrace sequences among the different river systems. Seven terraces (T_1 to T_7) are identified in the study area, decreasing systematically in elevation (Figs. 6–8). Terraces T_1 , T_2 , T_3 , and T_6 are extensively developed along river valleys within the piedmont (Figs. 6 and 7). These four terraces are preserved as bedrock strath terraces within the anticlines, whereas they more commonly occur as fill terrace beyond the structures. In contrast, the bedrock terraces T_4 and T_5 are identified only within the anticlines where their preservation is likely due to rock uplift of these folds.

The highest terrace (T_1) is preserved along Manas River (Figs. 2, 6c and 8a), and laterally correlates with the F_1 alluvial fan sequence

(Figs. 6 and 7). This terrace comprises a strath that is overlain by 10–30 m of fluvial gravels and that are in turn capped by loess 20–40 m thick. Terrace T_1 commonly lies >100 m above the modern river (Fig. 8). The analysis of the loess/paleosol succession overlying the alluvial gravels and ESR ages of fan F_1 (Fig. 5a) to which T_1 is correlated implies that T_1 is formed at ~530 ka. Similarly, the terrace T_2 grades laterally to F_2 (Figs. 6 and 7a), implying a terrace age corresponding with F_2 . To the south of fault-and-fold zone II, terraces T_3 and T_6 mainly developed as strath surfaces (Figs. 2 and 7) that grade downstream to alluvial fans F_3 and F_4 , respectively (Fig. 7). OSL ages (Fig. 8c and Table 2) and some previous studies (Molnar et al., 1994; Yuan et al., 2006) indicate that the age of terrace T_3 is ~10–30 ka. Terrace T_6 is inferred to have formed during the early Holocene. The bedrock terraces T_4 and T_5 are preserved only within anticlines where rock-uplift rates were apparently rapid enough to raise the strath above the active river. Terraces T_4 and T_5 are estimated to have formed during the latest Pleistocene (Xu et al., 1992b; Shi et al., 2004). Terrace T_7 is continuously developed in each active river valley with its height above the modern river diminishing downstream.

5. Discussion

Some previous studies (e.g., Zhang et al., 1995; Deng et al., 2000) argued that three continuous terraces characterize Quaternary fluvial geomorphic evolution within the north piedmont of the Tian Shan. Here we present a new division of seven fluvial terraces (T_1 to T_7). The most prominent and widely preserved terraces T_1 , T_2 , T_3 , and T_6 grade laterally or downstream to alluvial fans F_1 to F_4 , respectively. Based mainly on the terrace surface characteristics, their distribution, and the overlying loess/paleosol sequences, we conclude that terraces T_2 , T_3 and T_6 in this study are equivalent to terraces III, II and I named by Zhang et al. (1995), respectively. These three river terraces have been dated by thermoluminescence (Xu et al., 1992b; Wang and Wang, 2000), OSL, radiocarbon (Yuan et al., 2006), and cosmogenic nuclides dating (Molnar et al., 1994). However, significant discrepancies exist among those dates. Given that most previous studies on fluvial terraces focused on a single river system in the north piedmont of the Tian Shan, these differences may be due to the inability to make temporal comparisons among fluvial terrace sequences of different river systems (Xu et al., 1992b; Yang et al., 1995; Wang and Wang, 2000; Shi et al., 2004; Yuan et al., 2006) or from the lack of reliable ages for fluvial sequences and related deposits (e.g., Zhang et al., 1995). Our new chronology suggests that, following intervals of aggradation, river terraces (T_1 , T_2 and T_3) and equivalent alluvial fans (F_1 , F_2 and F_3) were abandoned at ~530 ka, ~300 ka and ~10 ka, respectively. Although some previous studies (e.g., Molnar et al., 1994; Zhang et al., 1995; Poisson and Avouac, 2004) have already proposed climatically forced formation of Quaternary fluvial geomorphology within the north piedmont of the Tian Shan, ambiguity has persisted concerning the correlations of river deposition and incision events to the established glacial phases of the north Tian Shan. These new age data presented above permit us to propose new correlations of alluvial fan deposition and terrace formation to climatic changes during glacial–interglacial transitions as below.

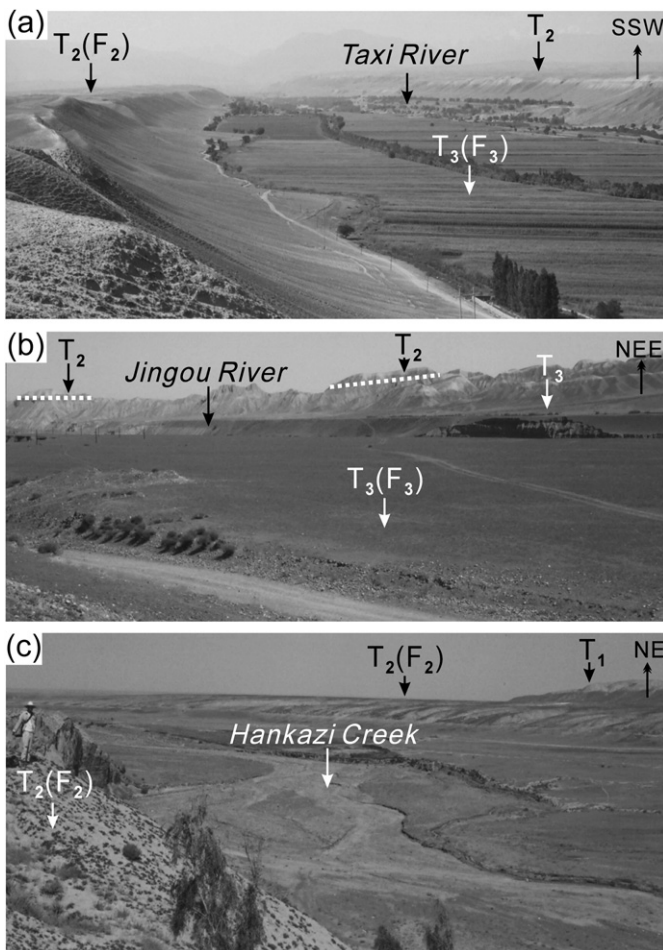


Fig. 6. Photos showing the lateral correlation of fluvial terraces to alluvial fans. (a) Taxi River; (b) Jingou River; and (c) Manas River.

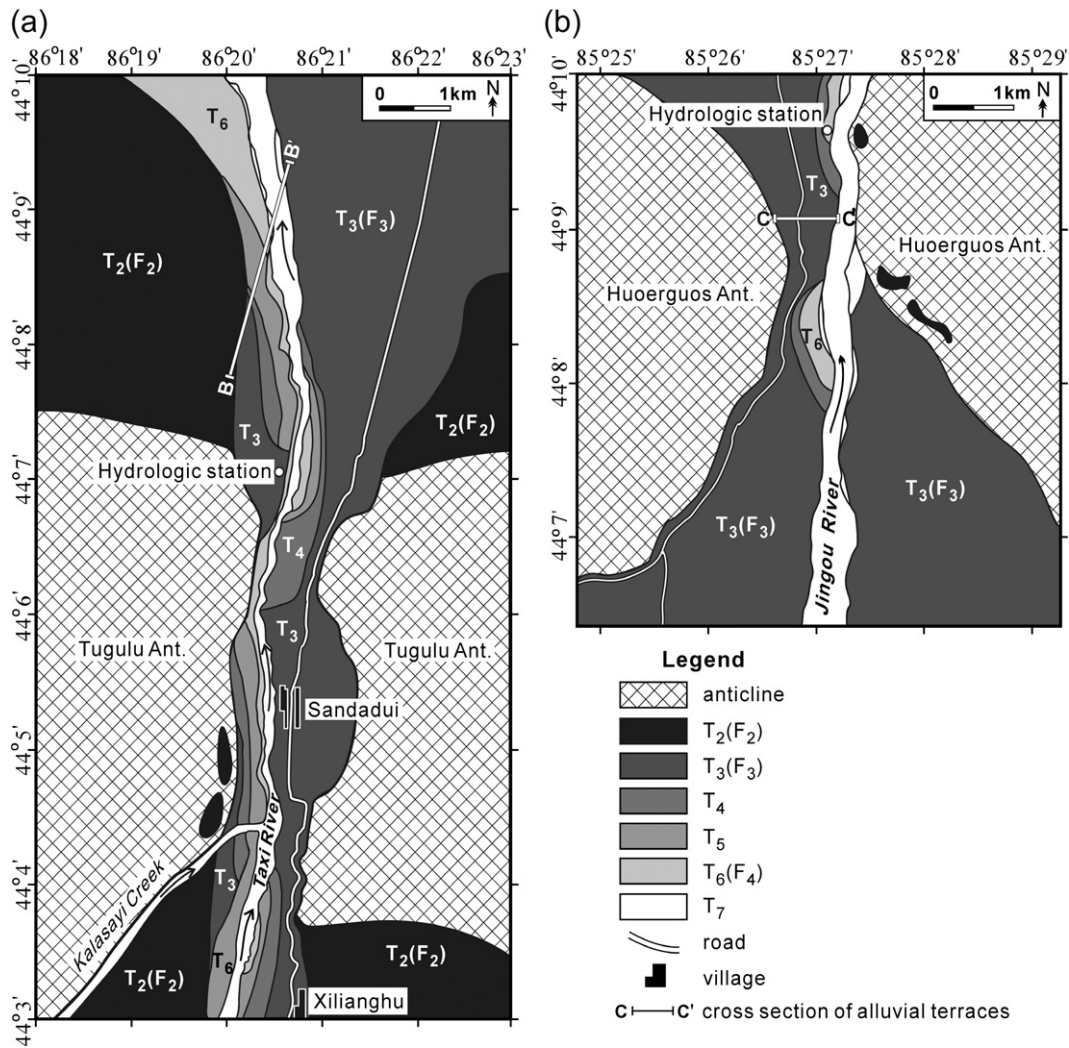


Fig. 7. Distribution of river terraces based on 1:50,000 topographic maps and field investigations. (a) Taxi River and (b) Jingou River. Terraces T_2 , T_3 , and T_6 grade laterally or downstream to alluvial fans F_2 , F_3 , and F_4 , respectively. See Fig. 2 for the location of Fig. 7.

The deposition of ~10–30 m of T_1 gravels on the underlying strath terrace prior to ~530 ka indicates that a lateral beveling event (strath formation) was followed by an increase in the relative sediment supply that drove aggradation. The T_1 aggradational surface was subsequently abandoned just prior to the development of the S_{5a} interglacial (MIS stage 13) paleosol (Figs. 3 and 5). The stabilization of the terrace surface allowed ~1.0 m of loess to accumulate on the terrace tread, and this loess layer was subsequently weathered to form the S_{5a} paleosol. Hence, we interpret that aggradation occurred late within a glacial phase and that incision began near the glacial–interglacial transition. This sequence of events with respect to climate change is comparable to that described for multiple terraces along the northern flank of the Tibetan Plateau (Pan et al., 2003). The glacial phase may be equivalent with the Hongshanzui ice age in the northern Tian Shan, the occurrence of which was estimated as within the early Middle Pleistocene (Xinjiang Institute of Geography, 1986).

Our data indicate that the formation of the T_2 terrace followed an analogous pattern. Above a bedrock strath, ~10–20 m of gravels accumulated before the aggradational surface was abandoned as the river began to incise. Subsequently, a small amount of loess (<1 m) was deposited on the terrace tread and then a paleosol (S_3) developed in that loess (Fig. 5b). The age of this basal interglacial paleosol suggests that the gravel aggradation may have occurred during the Haxiongou ice age (Xinjiang Institute of Geography, 1986) in the northern Tian Shan, just prior to MIS 9 at ~300 ka.

The OSL dates of the terrace T_3 (the F_3 fan) (Table 2 and Fig. 8c) suggest a beginning of aggradation at ~26–28 ka and an abandonment of the terrace at ~12 ka. Aggradation persisted at least a period of ~15 kyr during the latter part of the last glaciation and into the deglacial phases. Aggradation ended as the river began to incise by ~10 ka. Given the terrace chronology presented here, we infer that the absence of fluvial terraces attributable to the Hustai glacial–interglacial transition (equivalent with MIS 2 to 4) during earliest Late Pleistocene (Xinjiang Institute of Geography, 1986) may result from intensive lateral beveling by the piedmont rivers prior to the creation of the T_3 terrace.

We interpret the above correlations to define a clear causal relationship between river incision and climate change during the glacial–interglacial transition within the north piedmont of the Tian Shan. Undeniably, tectonic uplift may be also involved as a controlling factor in fluvial process (e.g., Li et al., 1996, 1999; Lu et al., 2004; Sun, 2005), especially in a tectonically active regime. Main deposition and incision events in the present study area, however, are not regarded as tectonically controlled based on the following evidences.

First, clear effects of tectonic activity are only expressed topographically within deformed and uplifted structure zones several kilometers wide, corresponding to growing anticlines: strath terraces have been warped and faulted within these zones (e.g., Avouac et al., 1993; Molnar et al., 1993; Zhang et al., 1994; Yang et al., 1995). In more extensive areas beyond anticlines, prevailing river incision

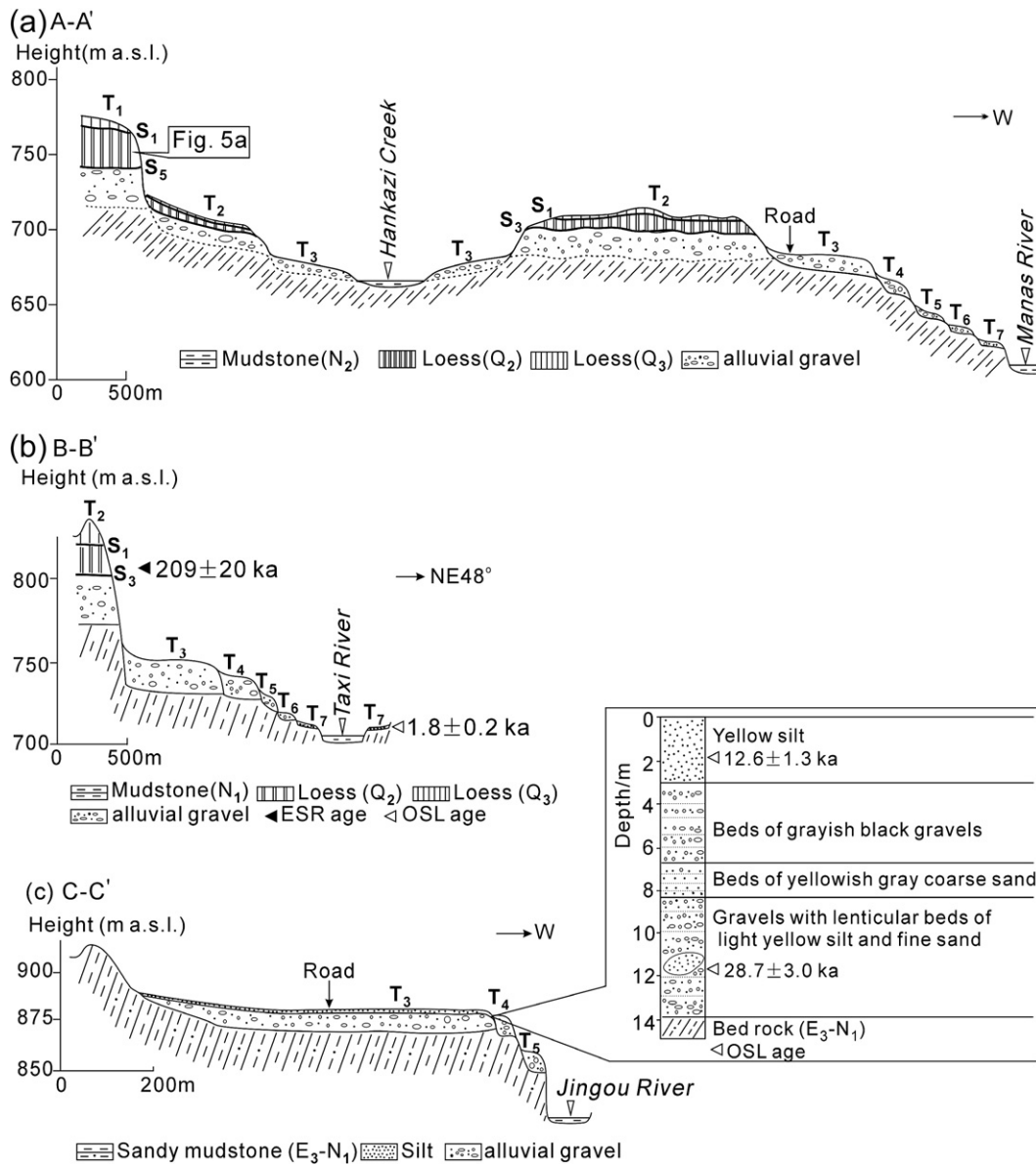


Fig. 8. Terrace-to-river cross-sections from the north piedmont of the Chinese Tian Shan. A–A': Manas River; B–B': Taxi River; C–C': Jingou River. See Figs. 2 and 7 for the locations of cross-sections. River terraces T₁, T₂, T₃, and T₆ are regionally developed, whereas terraces T₄ and T₅ are straths formed in the cores of active folds. See the text for the detailed description.

across the piedmont has yielded well-preserved fill terraces, whereas thick alluvial deposits indicate subsidence between structure zones with respect to uplifting anticlines. Second, the contribution of tectonic activity to fluvial incision in the northern Tian Shan foreland is relatively small in comparison to the magnitude of downcutting. At Kuitun He (He is Mandarin for “river”), tectonic uplift of Dushanzi anticline due to thrusting and folding only accounts for about 10% of total incision of ~300 m (Poisson and Avouac, 2004). At Taxi He, rock uplift over the last 300 kyr of the core of the Tugulu anticline is estimated to be ~130 m based on topographic surveys of the oldest river terrace III (Terrace T₂ in this study) preserved along this river system (Deng et al., 2000). Even in the core of the anticline, this magnitude of rock uplift is <50% of the total incision (~280 m) during this same period. The simplest interpretation of this scenario is that tectonic deformation documented by deformed Quaternary terraces has contributed little to specific events of terrace creation across the piedmont, especially beyond structure zones. Finally, if, as is seen with the dated terraces in this study (such as terrace T₂ and the correlative fan F₂), the age of a given terrace is approximately synchronous

among multiple folds at different positions within foreland thrust belts. Such synchrony is consistent with regional climatic control on depositional regimes, rather than with synchronous changes in folding and rock-uplift rates across the foreland. Whereas the multi-level terrace-and-fan system argues for pulsed controls on sediment fluxes and fluvial incision regimes, studies of deformed terraces (Molnar et al., 1993) suggest a steady, rather than a pulsed, folding.

Within the north piedmont of the Tian Shan, however, basinward thrusting of the Tian Shan range (Molnar and Tapponnier, 1975; Avouac et al., 1993; Deng et al., 2000; Lu et al., 2009) could have driven rock uplift of the headwaters of those piedmont rivers with respect to Junggar Basin to the north. Such uplift might have caused overall downcutting in response to a more steepened gradient. Consequently, climatically forced incision, especially during the rhythmic climatic fluctuations of the Quaternary, could be the specific “noise” in a long-term-downcutting regime driven by tectonism across the entire region. The likely primacy of climatic controls has emerged from several other regional studies, e.g., Poisson and Avouac, 2004; Starkel, 2003; and Pan et al., 2003. In the north piedmont of the

Tibetan Plateau, the terrace chronology supports the contention of Pan et al. (2003) that formation of paired terraces over the past 900 kyr were responses to climate changes during glacial–interglacial transitions despite the ongoing tectonic deformation indicated by faulted terraces.

6. Conclusions

A combination of geomorphological, stratigraphic, and chronologic criteria underpins a new division of the Quaternary alluvial sequence in the northern piedmont of the Tian Shan. ESR and OSL geochronologies and loess/paleosol stratigraphic correlations provide a robust chronologic framework for these regional alluvial units. Three main river terraces (terraces T_1 to T_3), correlating with alluvial fans F_1 to F_3 , respectively, are dated at ~530 ka, ~300 ka, and ~10 ka, respectively. Together with basal paleosol layers in the loess sequences that directly overlie two older terraces (T_1 and T_2) and fans (F_1 and F_2), this new chronology suggests that the gravel aggradation persisted until late in the glacial cycles and that the subsequent incision that caused abandonment/stabilization of these terraces and fans occurred near the glacial–interglacial transitions. Therefore, we argue that climate changes during glacial–interglacial transitions have driven changes from aggradation or strath formation to river incision in the north piedmont of the Tian Shan. These regional alluvial sequences are largely decoupled from the locally folded and faulted river terraces that define ongoing, but spatially restricted tectonic activity. Given the limited dates presented in this study, our identification of the F_2 fan as a regionally synchronous feature remains somewhat uncertain. Future work should focus (1) on the middle part of the northern Tian Shan foreland in order to better constrain the cessation of the F_2 fan deposition and (2) on detailed chronologies of terrace aggradation and abandonment to further test climate–terrace linkages.

Acknowledgments

Honghua Lu gives the special appreciation to China Scholarship Council (CSC) who supported him to study at the University of California, Santa Barbara, USA. We thank Hongya Wang for the assistance in the magnetic susceptibility testing and Jie Chen for the ESR and OSL dating. Supei Si, Yunming Liu and Hongzhuang Zhao are especially appreciated for their field assistance. Discussions with Jingchun Yang were helpful and appreciated. We wish to thank two anonymous reviewers and the editor A. Peter Kershaw who refereed this paper for their very thoughtful and thorough reviews. This study was financially supported by National Natural Science Foundation of China (Grant 40971001), the US National Science Foundation (EAR 0230403), and China Postdoctoral Science Foundation (Grant 20090450727).

References

Abdrakhmatov, K.Y., Aldazhanov, S.A., Hager, B.H., Hamburger, M.W., Herring, T.A., Kalabaev, K.B., Makarov, V.I., Molnar, P., Panasyuk, S.V., Prilepin, M.T., Reilinger, R.E., Sadybakasov, I.S., Souter, B.J., Trapeznikov, Y.A., Tsurkov, V.Y., Zubovich, A.V., 1996. Relatively recent construction of the Tien Shan inferred from GPS measurements of present-day crustal deformation rates. *Nature* 384, 450–453.

An, Z.S., Liu, T.S., Lu, Y.C., 1990. The long-term paleomonsoon variation recorded by the loess–paleosol sequence in central China. *Quaternary International* 7–8, 91–95.

An, Z.S., Kukala, G., Proter, S.C., 1991. Late Quaternary dust flow on the Chinese loess plateau. *Catena* 18, 125–132.

Avouac, J.-P., Tapponnier, P., Bai, P., You, M., Wang, G., 1993. Active thrusting and folding along the northern Tien Shan and late Cenozoic rotation of the Tarim relative to Dzungaria and Kazakhstan. *Journal of Geophysical Research* 98 (B4), 6755–6804.

Avouac, J.-P., Peltzer, G., 1993. Active tectonics in Southern Xinjiang, China. *Journal of Geophysical Research* 98 (B12), 21773–21807.

Bridgland, D., Westaway, R., 2007. Climatically controlled river terrace staircases: a world-wide Quaternary phenomenon. *Geomorphology*. doi:10.1016/j.geomorph.2006.12.032.

Burchfiel, B.C., Brown, E.T., Deng, Q., Feng, X., Li, J., Molnar, P., Shi, J., Wu, Z., You, H., 1999. Crustal shortening on the margins of the Tien Shan, Xinjiang, China. *International Geology Review* 41 (8), 665–700.

Charreau, J., Chen, Y., Gilder, S., Dominguez, S., Avouac, J.-P., Sen, S., Sun, D., Li, Y., Wang, W., 2005. Magnetostratigraphy and rock magnetism of the Neogene Kuitun He section (northwest China): implications for Late Cenozoic uplift of the Tianshan mountains. *Earth and Planetary Science Letters* 230, 177–192.

Charreau, J., Gilder, S., Chen, Y., Dominguez, S., Avouac, J.-P., Sen, S., Jolivet, M., Li, Y., Wang, W., 2006. Magnetostratigraphy of the Yaha section, Tarim Basin (China): 11 Ma acceleration in erosion and uplift of the Tian Shan Mountains. *Geology* 34 (3), 181–184.

Chen, J., Heermance, R., Burbank, D.W., Scharer, K.M., Miao, J., Wang, C., 2007. Quantification of growth and lateral propagation of the Kashi anticline, southwest Chinese Tian Shan. *Journal of Geophysical Research* 112. doi:10.1029/2006JB004345.

Deng, Q.D., Feng, X.Y., Zhang, P.Z., Xu, X.W., Yang, X.P., Peng, S.Z., Li, J., 2000. Active tectonics of the Tian Shan Mountains. *Seismology Press, Beijing*, 399 pp. (in Chinese).

Ding, Z.L., Yu, Z.W., Rutter, N.W., 1994. Towards an orbital time scale for Chinese loess deposits. *Quaternary Science Reviews* 13, 39–70.

Fang, X.M., Shi, Z.T., Yang, S.L., Li, J.J., Jiang, P.A., 2002. Loess sediments in the north piedmont of Tian Shan and its implication for the development of the Guerbantonggute desert. *Chinese Science Bulletin* 47 (7), 540–545 (in Chinese).

Fu, B., Lin, A., Kano, K.-I., Maruyama, T., Guo, J., Abdrakhmatov, K.Y., 2003. Quaternary folding of the eastern Tian Shan, northern China. *Tectonophysics* 369, 79–101.

Hanson, P.R., Mason, J.A., Goble, R.J., 2006. Fluvial terrace formation along Wyoming's Laramie Range as a response to increased late Pleistocene flood magnitudes. *Geomorphology* 76, 12–25.

Heermance, R.V., Chen, J., Burbank, D.W., Wang, C.S., 2007. Chronology and tectonic controls of Late Tertiary deposition in the southwestern Tian Shan foreland, NW China. *Basin Research* 19, 599–632.

Kukla, G., Heller, F., Liu, X.M., Xu, T.C., Liu, T.S., An, Z.S., 1988. Pleistocene climates in China dated by magnetic susceptibility. *Geology* 16, 811–814.

Li, J.J., Fang, X.M., Ma, H.Z., Zhu, J.J., Pan, B.T., Chen, H.L., 1996. Geomorphological evolution in the upper reaches of the Yellow River during the late Cenozoic and its implication for the uplift of the Tibet Plateau. *Science in China (Series D)* 26 (4), 316–322 (in Chinese).

Li, Y.L., Yang, J.C., 1997. Response of alluvial terraces to Holocene climatic changes in the Hexi Corridor basins, Gansu, China. *Scientia Geographica Sinica* 13 (3), 248–252 (in Chinese, with English abstract).

Li, Y.L., Yang, J.C., Tan, L.H., Duan, F.J., 1999. Impact of tectonics on alluvial landforms in Hexi Corridor, Northwest China. *Geomorphology* 28, 229–308.

Lin, M., Jia, L., Ding, Y., Cui, Y., Cheng, K., Li, H., Xiao, Z., Ying, G., 2005. Dose determination in ESR dating research. *Seismology and Geology* 27 (4), 698–705 (in Chinese, with English abstract).

Lisiecki, L.E., Raymo, M.E., 2005. A Pliocene–Pleistocene stack of 57 globally distributed benthic $\delta^{18}\text{O}$ records. *Paleoceanography* 20, PA1003. doi:10.1029/2004PA001071.

Liu, T.S., 1965. Loess Sediments in China. *Science Press, Beijing* (in Chinese).

Liu, T.S., 1985. Loess and the Environment. *China Ocean Press, Beijing* (in Chinese).

Liu, T.S., Zhang, Z.G., 1962. Loess in China. *Acta Geologica Sinica* 42 (1), 1–14 (in Chinese).

Lu, H.Y., An, Z.S., Wang, X.Y., Tang, H.B., Zhu, R.X., Ma, H.Z., Li, Z., Miao, X.D., Wang, X.Y., 2004. Geomorphic evidences of uplift of northeastern Qihai-Xizang plateau since 14 Ma B.P. *Science in China (Series D)* 34 (9), 855–864 (in Chinese).

Lu, H.H., Burbank, D.W., Li, Y.L., Liu, Y.M., 2009. Late Cenozoic structural and stratigraphic evolution of the northern Chinese Tian Shan foreland. *Basin Research*. doi:10.1111/j.1365-2117.2009.00412.x.

Macklin, M.G., Fuller, I.C., Lwein, J., Maas, G.S., Passmore, D.G., Rose, J., Woodward, J.C., Black, S., Hamlin, R.H.B., Rowan, J.S., 2002. Correlation of fluvial sequences in the Mediterranean basin over the last 200 ka and their relationship to climate change. *Quaternary Science Reviews* 21 (14–15), 1633–1641.

Molnar, P., Tapponnier, P., 1975. Cenozoic tectonics of Asia: effects of a continental collision. *Science* 189, 419–426.

Molnar, P., England, P., Martinod, J., 1993. Mantle dynamics, uplift of the Tibetan Plateau, and the Indian monsoon. *Reviews of Geophysics* 31 (4), 357–396.

Molnar, P., Brown, E.T., Burchfiel, B.C., Deng, Q.D., Feng, X.Y., Li, J., Raisbeck, G.M., Shi, J.B., Wu, Z.M., You, H.C., 1994. Quaternary climate change and the formation of river terraces across growing anticlines on the north flank of the Tien Shan, China. *Journal of Geology* 102, 583–602.

Pan, B.T., Burbank, D.W., Wang, Y.X., Wu, G.J., Li, J.J., Guan, Q.Y., 2003. A 900 k.y. record of strath terrace formation during glacial–interglacial transitions in northwest China. *Geology* 31 (11), 957–960.

Pinter, N., Keller, E.A., West, R.B., 1994. Relative dating of terraces of the Owens River, northern California, and correlation with moraines of the Sierra Nevada. *Quaternary Research* 42, 266–276.

Poisson, B., Avouac, J.-P., 2004. Holocene hydrological changes inferred from alluvial stream entrenchment in North Tian Shan (Northwestern China). *Journal of Geology* 112, 231–249.

Pratt, B., Burbank, D.W., Heimsath, A., Ojha, T., 2002. Impulsive alluviation during early Holocene strengthened monsoons, central Nepal Himalaya. *Geology* 30, 911–914.

Reigber, C., Michel, G.W., Galas, R., Angermann, D., Klotz, J., Chen, J.Y., Papschev, A., Arslanov, R., Tzurkov, V.E., Ishanov, M., 2001. New space geodetic constraints on the distribution of deformation in Central Asia. *Earth and Planetary Science Letters* 91, 157–165.

Rees-Jones, J., 1995. Optical dating of young sediments using fine-grain quartz. *Ancient TL* 13 (2), 9–14.

Scharer, K.M., Burbank, D.W., Chen, J., Weldon II, R.J., 2006. Kinematic models of fluvial terraces over active detachment folds: constraints on the growth mechanism of the Kashi-Atushi fold system, Chinese Tian Shan. *Geological Society of America Bulletin* 118 (7–8), 1006–1021.

Shi, X.M., Yang, J.C., Li, Y.L., Nan, F., 2004. Deformation of Manas River terraces and neotectonics in the north flank of the Tian Shan Mountains. *Acta Scientiarum*

- Naturalium Universitatis Pekinensis 40 (6), 971–978 (in Chinese, with English abstract).
- Starkel, L., 2003. Climatically controlled terraces in uplifting mountain areas. *Quaternary Science Reviews* 22, 2189–2198.
- Sun, J., 2005. Long-term fluvial archives in the Fen Wei Graben, central China, and their bearing on the tectonic history of the India–Asia collision system during the Quaternary. *Quaternary Science Reviews* 24 (10–11), 1279–1286.
- Suppe, J., Chou, G.T., Hook, S.C., 1992. Rates of folding and faulting determined from growth strata. In: McClay, K.R. (Ed.), *Thrust Tectonics*. Chapman & Hall, Suffolk, pp. 105–121.
- Tapponnier, P., Xu, Z., Roger, F., Meyer, B., Arnaud, N., Wittlinger, G., Yang, J., 2001. Oblique stepwise rise and growth of the Tibetan Plateau. *Science* 294, 1671–1677.
- Wang, X.L., 2006. On the performances of the single-aliquot regenerative-dose (SAR) protocol for Chinese loess: fine quartz and polymineral grains. *Radiation Measurements* 41 (1), 1–8.
- Wang, Y., Wang, Y.B., 2000. Formation of Anjihai River terraces at the north Tian Shan piedmont, Xinjiang, and its significance. *Geological Review* 46 (6), 584–587 (in Chinese, with English abstract).
- Westaway, R., Bridgland, D., White, M., 2006. The Quaternary uplift history of central southern England: evidence from the terraces of the Solent River system and nearby raised beaches. *Quaternary Science Reviews* 25, 2212–2250.
- Xinjiang Institute of Geography, Chinese Academy of Sciences, 1986. *Evolutions of the Tianshan Mountains*. Science Press, Beijing, pp. 16–49. pp.80–116 (in Chinese).
- Xu, C.M., He, X.S., Wu, X.Z., Yao, X.Y., 1992a. Structure analysis and petroleum exploration prospect of Tostai area in Juggar Basin. *Xinjiang Petroleum Geology* 13 (3), 197–205 (in Chinese, with English abstract).
- Xu, X.W., Deng, Q.D., Zhang, P.Z., Feng, X.Y., Li, J., Wu, Z.M., Chen, J., Yang, X.P., Zhao, R.B., Tang, W., 1992b. Deformation of fluvial terraces across the Manas-Huoerguos reverse fault and fold zone and its neotectonic implication in Xinjiang, northwestern China. In: *Editing Committee of the Research of Active Fault* (Eds.), *Research of active fault* (II). Seismology Press, Beijing, pp.117–127 (in Chinese, with English abstract).
- Yang, J.C., Tan, L.H., Li, Y.L., Duan, F.J., 1998. River terraces and neotectonic evolution at the north margin of the Qilianshan Mountains. *Quaternary Science* 3, 229–237 (in Chinese, with English abstract).
- Yang, X.P., Deng, Q.D., Zhang, P.Z., Feng, X.Y., Peng, S.Z., 1995. Deformation of fluvial terraces across the Tugulu reverse fault-fold and its neotectonic implication in the northern flank of the Tian Shan Mountains. In: *Editing Committee of the Research of Active Fault* (Eds.), *Research of active fault* (IV). Seismology Press, Beijing, pp.46–62 (in Chinese, with English abstract).
- Yuan, Q.D., Guo, Z.J., Zhang, Z.C., Wu, C.D., Fang, S.H., 2006. The Late Cenozoic deformation of terraces on the north flank of Tian Shan Mountains and the tectonic evolution. *Acta Geologica Sinica* 80 (2), 210–216 (in Chinese, with English abstract).
- Zhang, P.Z., Deng, Q.D., Xu, X.W., Wu, Z.M., Yang, X.P., Feng, X.Y., Li, J., Chen, W., Zhao, R.B., Tang, W., 1994. Tectonic deformation, crustal shortening, and slip rate estimation along the Manas reverse fault-fold zone in the northern flank of the Tian Shan Mountains. In: *Editing Committee of the Research of Active Fault* (Eds.), *Research of Active Fault* (III). Seismology Press, Beijing, pp.18–32 (in Chinese, with English abstract).
- Zhang P.Z., Deng Q.Q., Yang X.P., Feng, X.Y., Peng, S.Z., Zhao, R.B., 1995. Glaciofluvial fan and neotectonic movement along the north piedmont of Tian Shan Mountains. In: *Editing Committee of the Research of Active Fault* (Eds.) *Research of Active Fault* (IV). Seismology Press, Beijing, pp.63–78 (in Chinese, with English abstract).
- Zhang, Y.L., 1981. Loess sediments in the north piedmont of Tian Shan. *Xinjiang Geology* 42 (1), 21–39 (in Chinese, with English abstract).
- Zhou, T.R., 1963. Quaternary terrestrial sediments and its relation with geomorphology and climate. *Acta Geographica Sinica* 29 (2), 109–129 (in Chinese, with English abstract).